CHAPTER 9
THE DYNAMIC PROCESS RESPONSE TO SOLIDIFICATION AND MELTING OF THE FREEZE LINING AND CRUST

The focus of this chapter is the influence of slag solidification and melting on the slag bath and, of secondary importance, on other parts of the process. A small number of experiments were conducted to specifically study slag solidification and melting in the crust region. The following aspects were considered:

- Freeze lining and crust thickness.
- Temperature distribution through the furnace wall, freeze lining and crust.
- Time lag in temperature response of the refractory brick wall relative to the time when conditions were changed in the slag bath.
- Liquid slag temperature.
- Composition distribution through the freeze lining and crust.
- Liquid slag composition.

In addition to the above list, metal bath composition data, off-gas composition data, heat loss data and reactor power data are also presented to provide a comprehensive set of results for each experiment.

9.1 EXPERIMENTAL SETUP

The experimental setup used in this chapter was exactly the same as the setup used in CHAPTER 8. Refer to paragraph 8.1 (page 214) for details. The feed rates of ilmenite and reductant was returned to the values used in CHAPTER 8 after the period of down time. The power set point was set to the values used in CHAPTER 8 plus the additional amount specified to melt away the crust during a specific experiment. The additional power was removed once the entire crust had disappeared.

9.2 EXPERIMENTS

The parameters that were varied over the series of experiments include the following:

- Duration for which the furnace was switched off.
- The electrical power applied to melt away the crust.

The furnace was switched off for 30 minutes in experiments 9.1 and 9.2. Once the furnace was switched back on, the power set point was increased to the electrical power input until the crust had been melted away. The same procedure was followed for experiments 9.3 and 9.4, except that the duration of furnace down time was increased to 60 minutes.

EXPERIMENT NO.	DURATION OF DOWN TIME	POWER APPLIED TO MELT AWAY CRUST
9.1	30 minutes	500 kW
9.2	30 minutes	1,000 kW
9.3	60 minutes	500 kW
9.4	60 minutes	1,000 kW

Table 24 – List of experiments conducted for CHAPTER 9.

9.3 EXPERIMENTAL RESULTS

The results of experiments conducted as part of this chapter was presented in exactly the same way as in CHAPTER 8. Refer to paragraph 8.3 (page 216) for details.

9.3.1 Experiment 9.1

DURATION OF DOWN TIME	POWER APPLIED TO MELT AWAY CRUST
30 minutes	500 kW

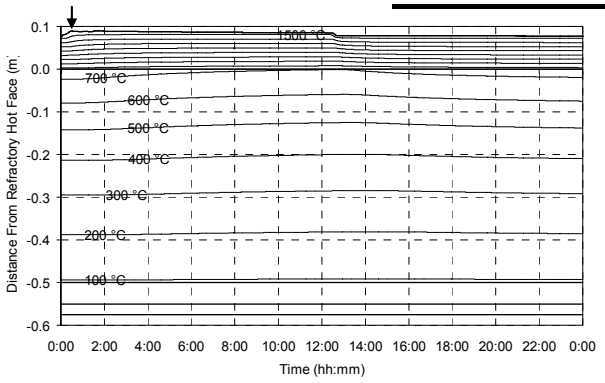

(a)

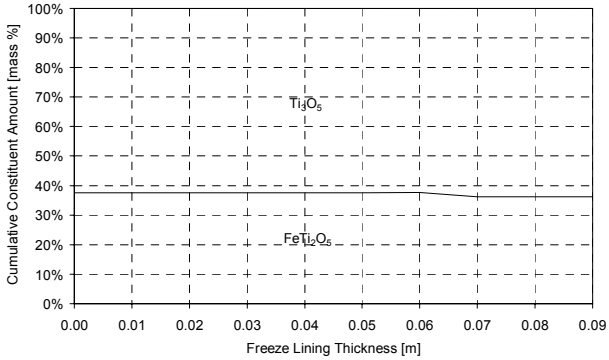

(b)

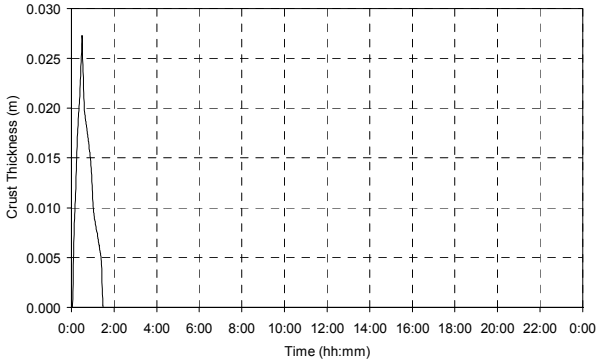

(c)

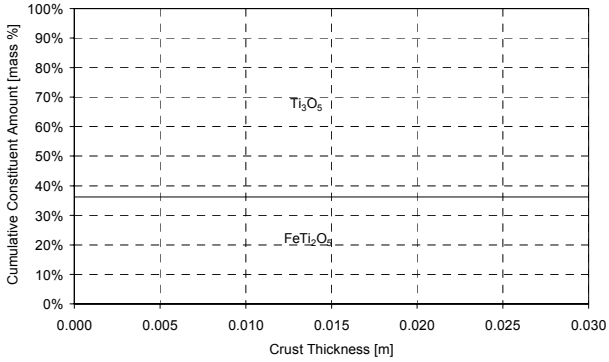

(d)

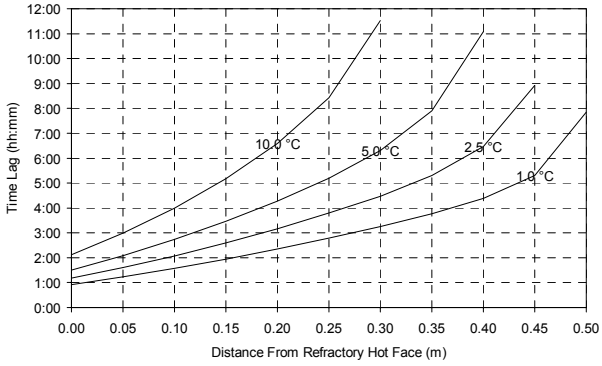

(e)

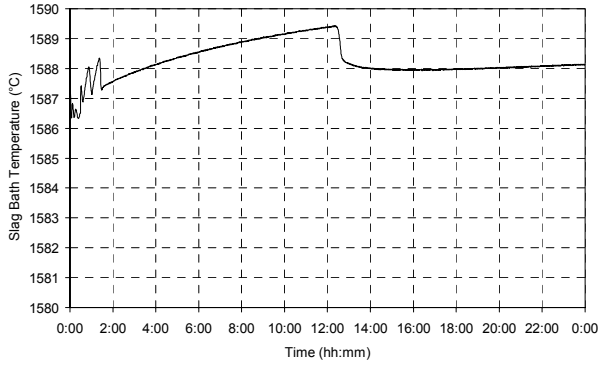

(f)

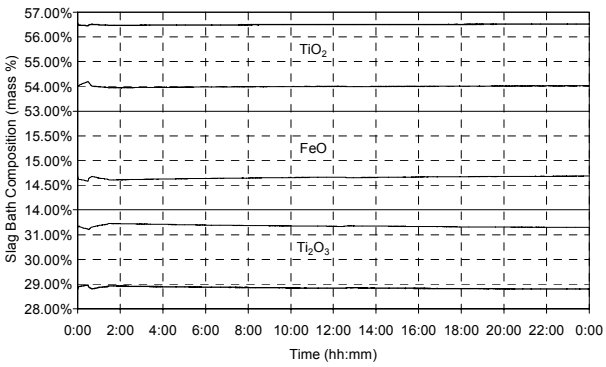

(g)

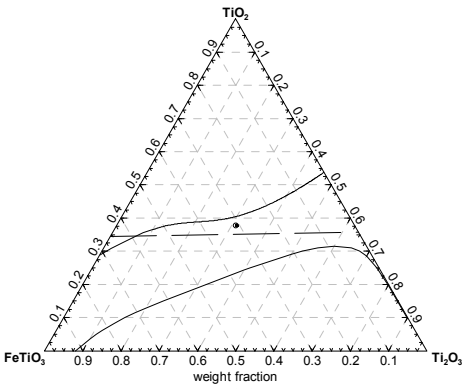

(h)

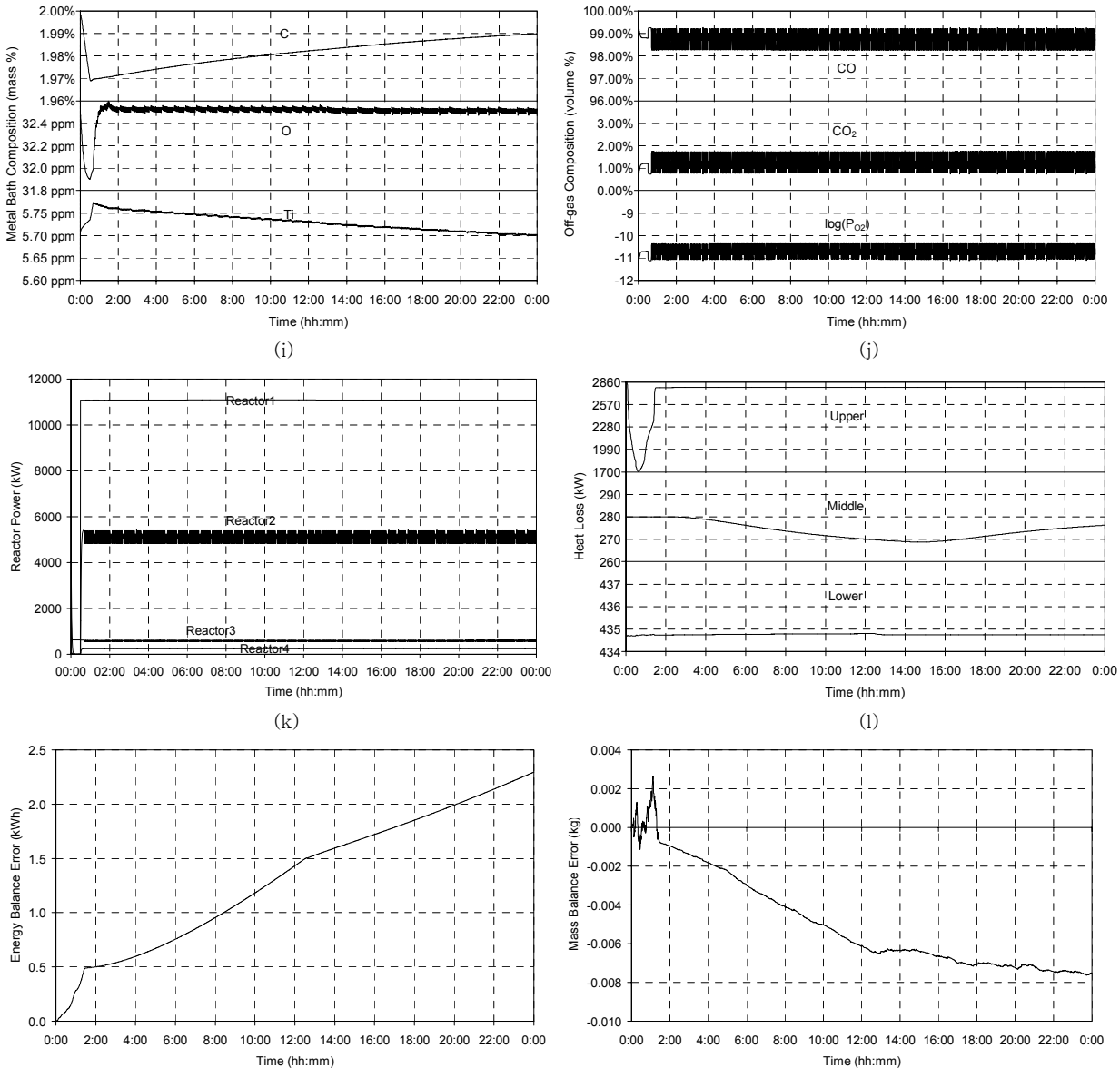

Figure 151 – Experiment 9.1 results.

9.3.2 Experiment 9.2

DURATION OF DOWN TIME	POWER APPLIED TO MELT AWAY CRUST
30 minutes	1,000 kW

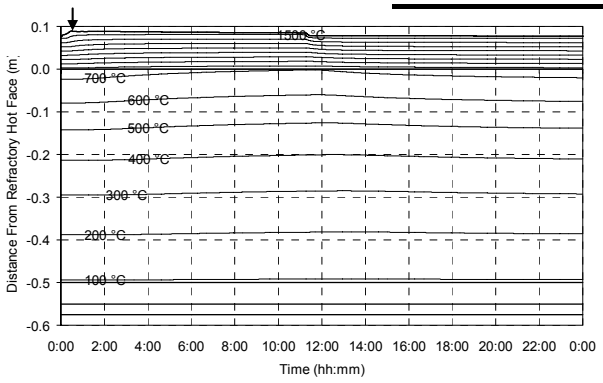

(a)

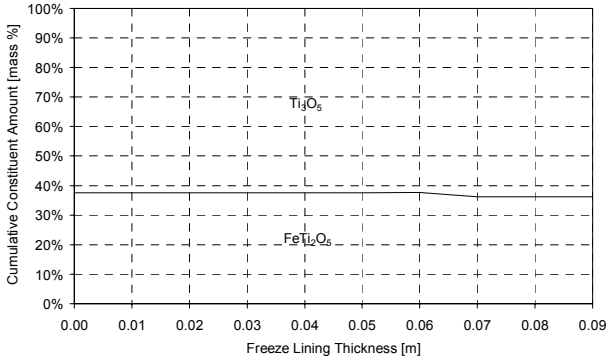

(b)

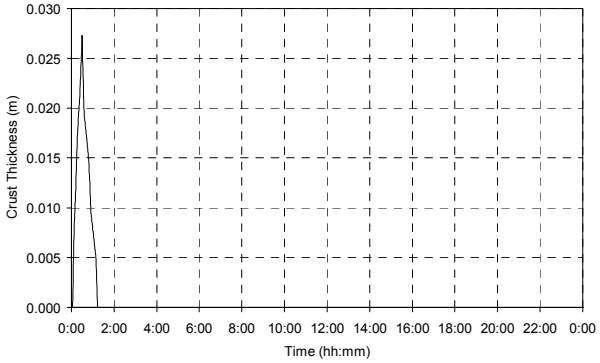

(c)

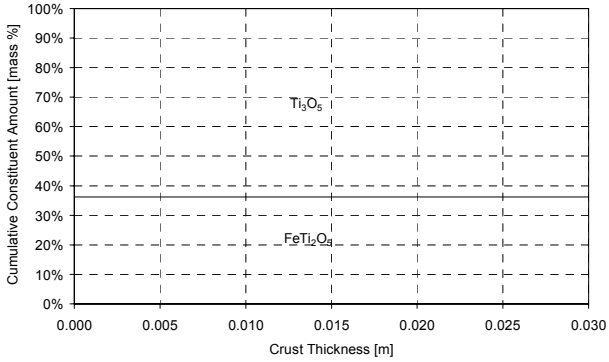

(d)

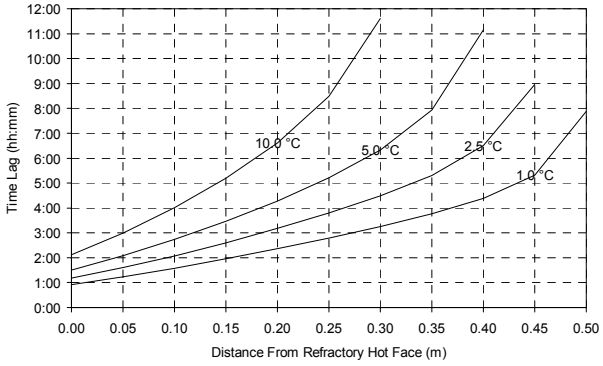

(e)

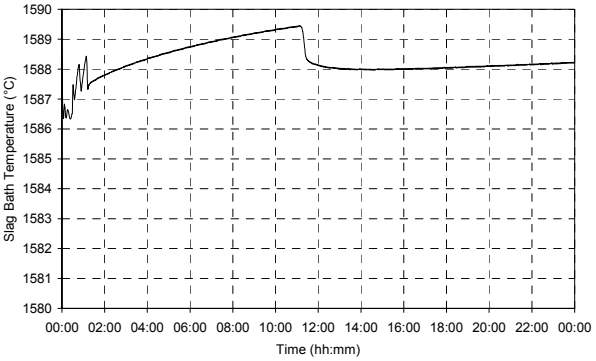

(f)

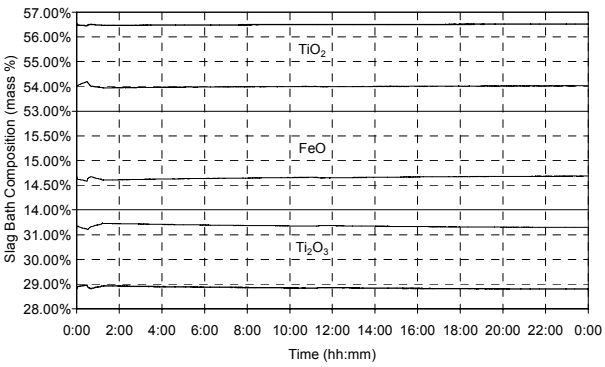

(g)

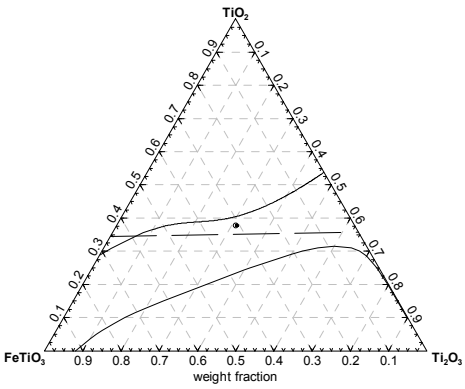

(h)

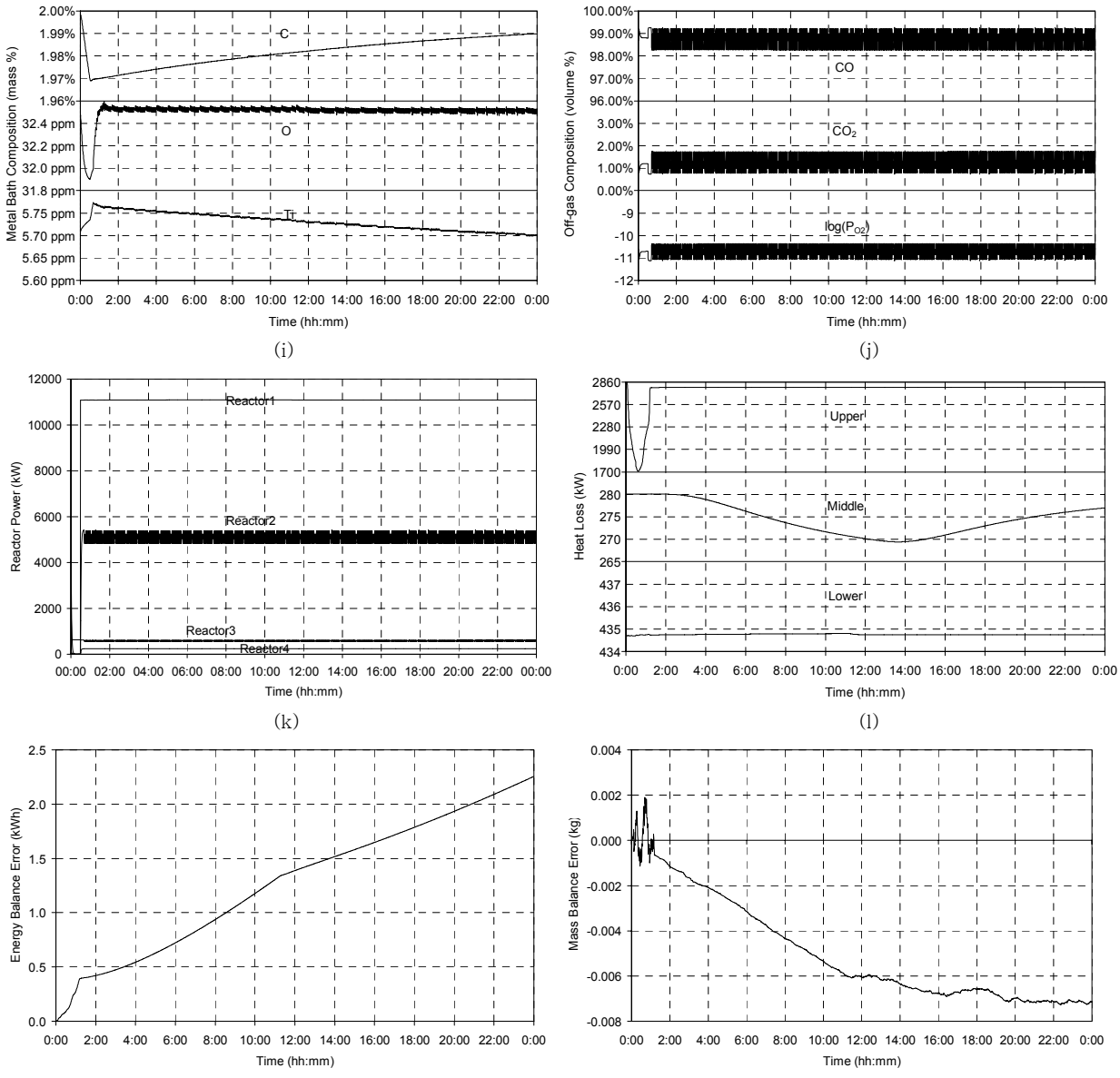

Figure 152 – Experiment 9.2 results.

9.3.3 Experiment 9.3

DURATION OF DOWN TIME	POWER APPLIED TO MELT AWAY CRUST
60 minutes	500 kW

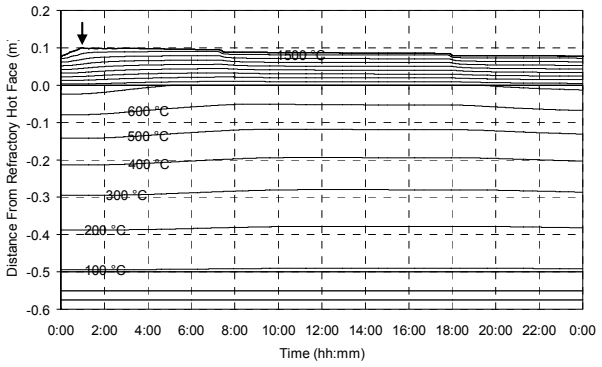

(a)

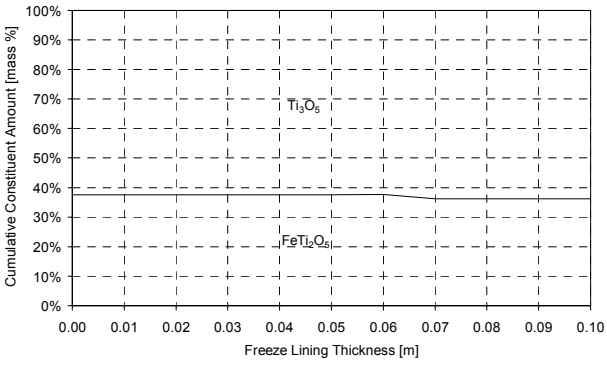

(b)

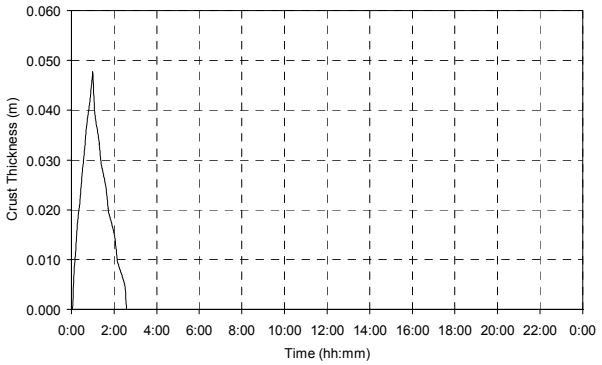

(c)

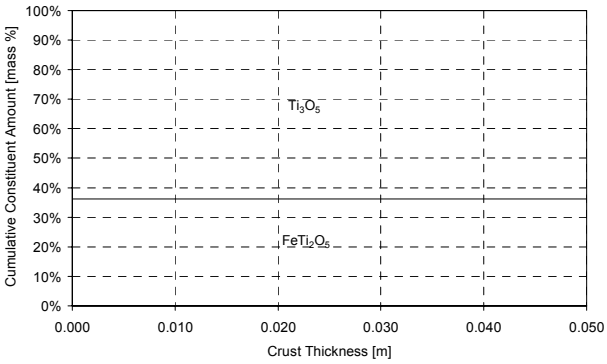

(d)

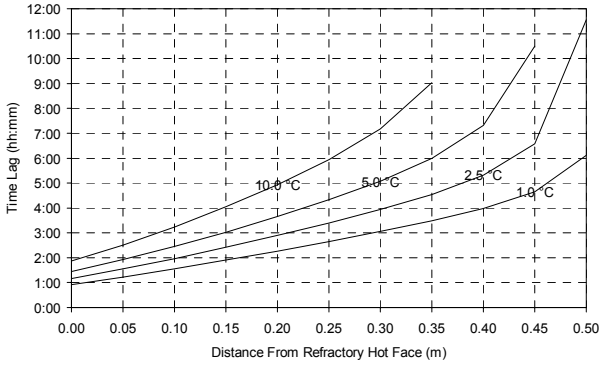

(e)

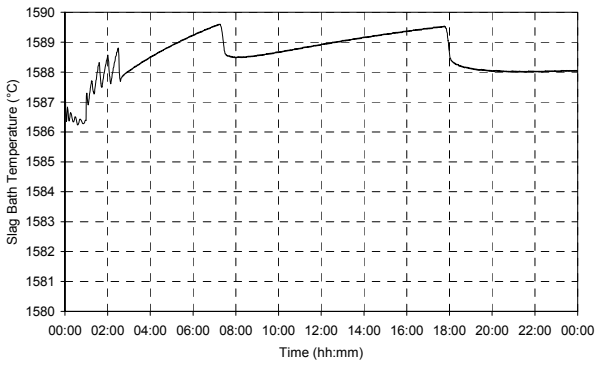

(f)

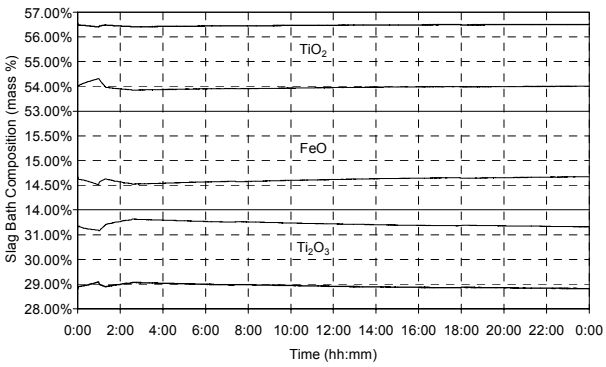

(g)

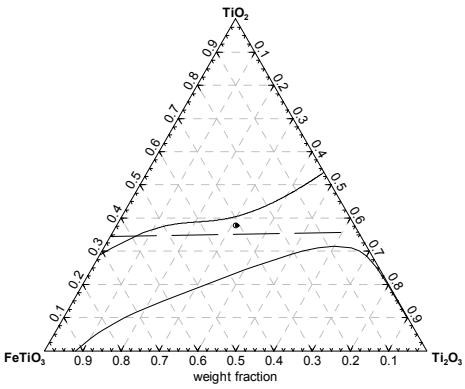

(h)

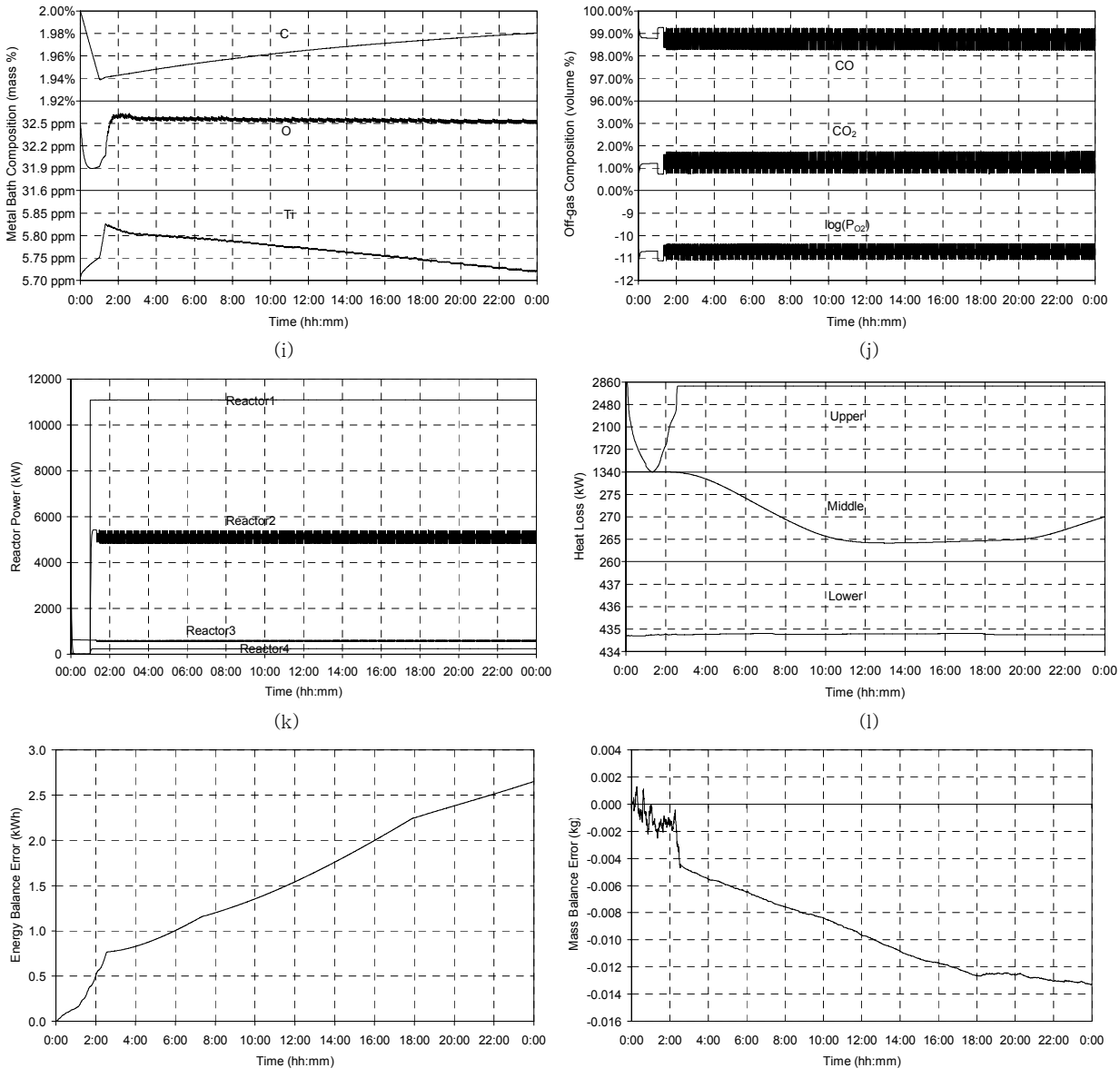

Figure 153 – Experiment 9.3 results.

9.3.4 Experiment 9.4

DURATION OF DOWN TIME	POWER APPLIED TO MELT AWAY CRUST
60 minutes	1,000 kW

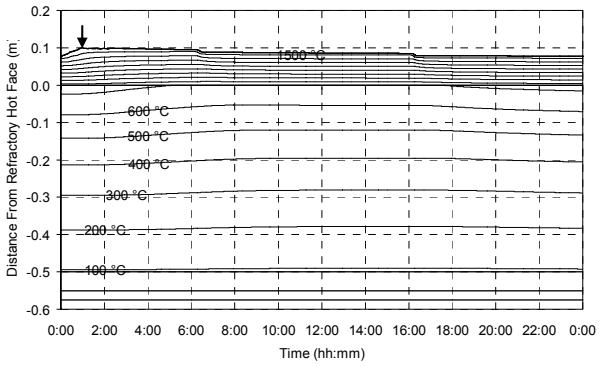

(a)

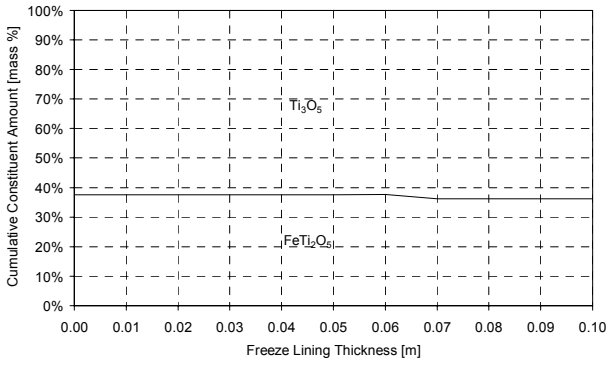

(b)

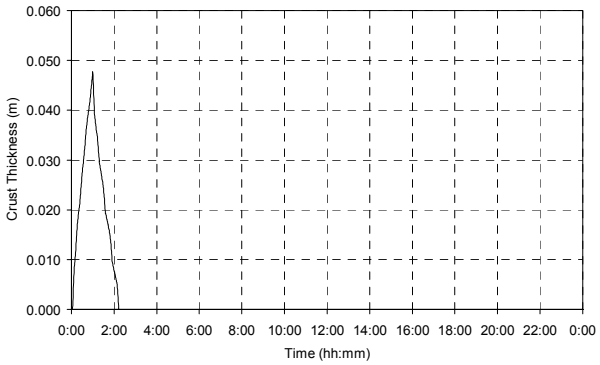

(c)

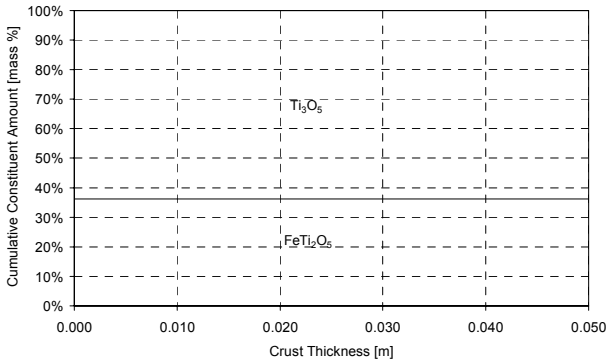

(d)

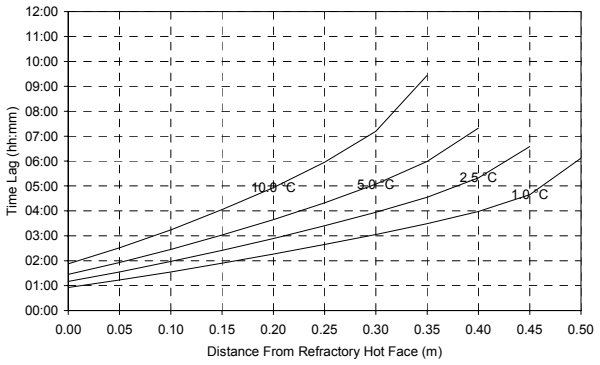

(e)

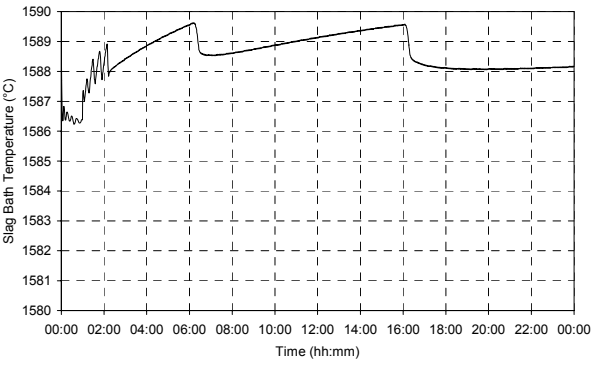

(f)

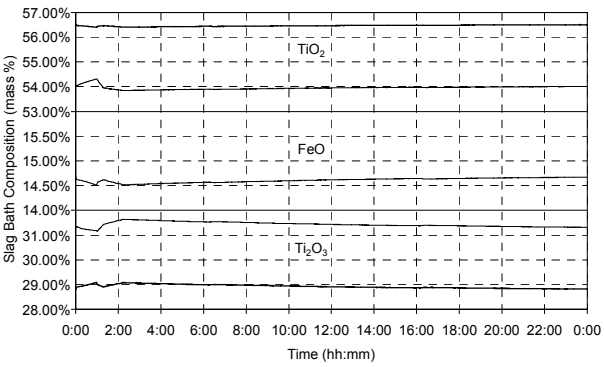

(g)

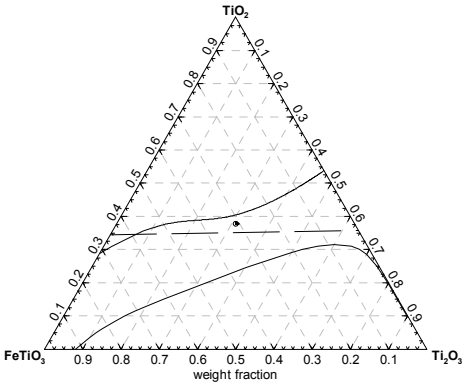

(h)

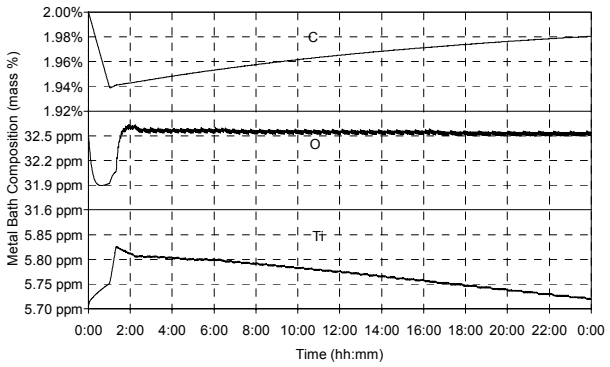

(i)

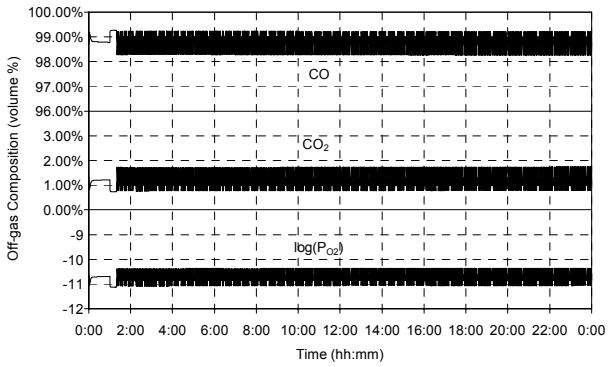

(j)

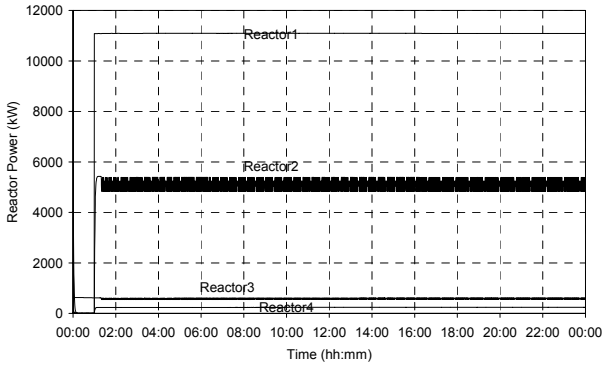

(k)

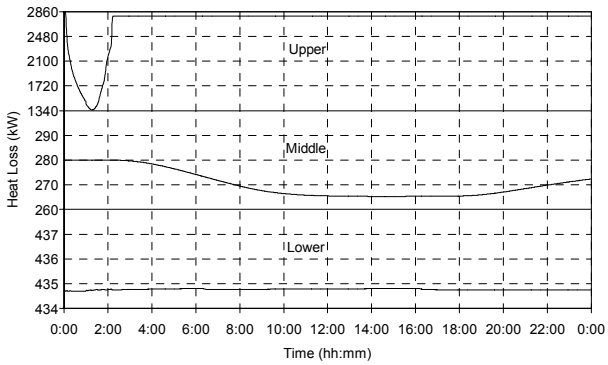

(l)

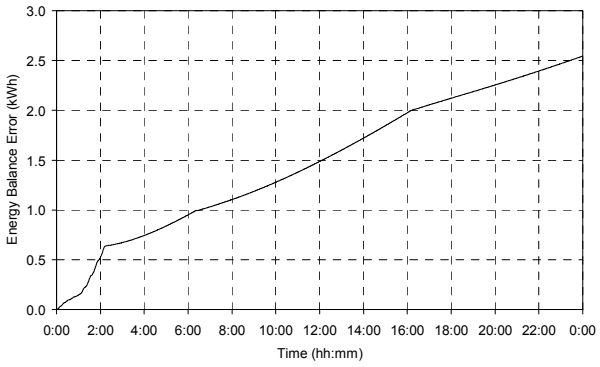

(m)

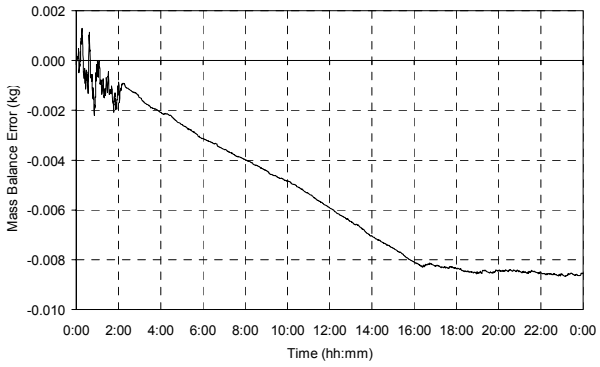

(n)

Figure 154 – Experiment 9.4 results.

9.4 DISCUSSION

9.4.1 Freeze Lining Thickness

Figure 155 presents the freeze lining thickness vs. time trends of experiments 9.1 to 9.4. This figure clearly shows the influence of the two adjusted variables (downtime duration and electrical power). Longer periods of downtime cause the freeze lining to grow thicker compared to shorter periods.

The higher electrical power (1000 kW) used during experiments 9.2 and 9.4 caused the freeze lining to return to its initial steady state thickness quicker than when the power was set to 500 kW. This was true even though this higher power set point was only employed while a crust was present.

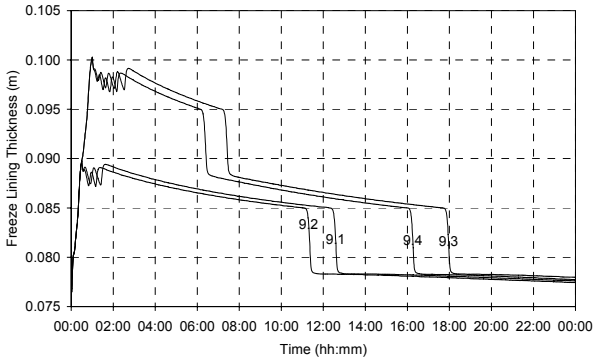

Figure 155 – Influence of downtime duration and electrical power on freeze lining thickness.

The step changes in freeze lining thickness in Figure 155 are the result of transitions from one finite difference node to the next. In reality these step changes will not occur, but the behaviour of an actual freeze lining should display the same tendencies as presented above.

9.4.2 Freeze Lining Composition

The freeze lining composition was plotted in graph (b) of the experimental results at its point of maximum thickness. Since this point occurred at the start of the experiment, these graphs do not assist in any form of interpretation. It is however expected that no significant variation in the freeze lining composition would have occurred because there was no great variation in liquid slag composition during any of the experiments. The composition of the freeze lining at its interface with the slag bath would also have been very similar to the crust composition as presented in graph (d).

9.4.3 Thermal Response of Freeze Lining and Furnace Wall

Graph (e) in the experimental results once again emphasises the slow thermal response of the furnace lining. A 1 °C change in temperature was only detected at the refractory hot face after 1 hour in all cases. The time required to detect a 1 °C change up to 0.25 m from the refractory hot face was roughly the same for all experiments.

The response during experiments 9.1 and 9.2 was virtually identical, as was the response during experiments 9.3 and 9.4. This indicates that the thermal response during these four experiments was

dominated by the downtime duration. The thermal response during the latter two experiments was in general quicker than the former two experiments. This is due to the larger temperature changes associated with longer downtime.

9.4.4 Crust Thickness

Figure 156 presents a summary of the variation of crust thickness with time for the four experiments conducted as part of this chapter.

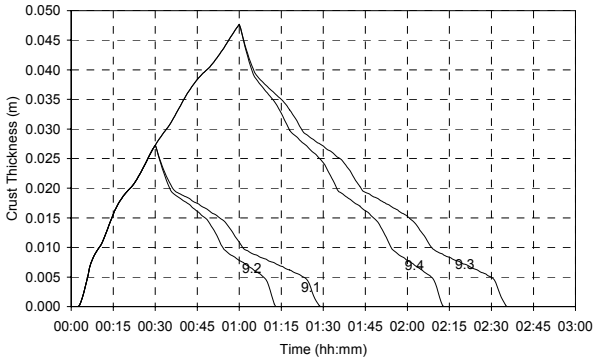

Figure 156 – Chapter 9 summary of crust thickness variation.

The influence of downtime duration is clear. A longer period of down time causes the crust to grow thicker. The rate at which the crust grows thicker however reduces with time. This is a result of a decline in the rate at which heat is extracted from the top of the crust as the crust grows thicker.

The influence of the electrical power set point on the rate at which the crust is melted away is also clear from Figure 156. A higher power input reduces the time required to melt away the crust. A thicker crust, as one would expect, takes longer to melt away.

When comparing experiment 9.1 with 9.2 or experiment 9.3 with 9.4, applying double the amount of extra power did not result in the time required to melt down the crust to reduce by 50%. The reason for this is that the extra power is applied to the entire process and not to the crust alone. Some of the extra power would therefore report as heat losses, some will contribute to melting of the freeze lining, some will melt down the crust, etc.

The volume fraction of solids in the slag bath can be calculated simply by dividing the crust thickness by the slag bath thickness (1 m). The solids content gives an indication of the effective slag viscosity.

9.4.5 Crust Composition

The crusts that formed during the four experiments consisted of only pseudobrookite. No rutile formed. The pseudobrookite was richer in Ti_2O_3 than the slag bath, as would be expected from the solidification behaviour that has been demonstrated in previous chapters.

9.4.6 Slag Bath Temperature

The variation of slag bath temperature for the four experiments is presented together in Figure 157. From this figure it is evident that the difference in temperature variation between the four experiments is minimal.

The oscillations of the temperature signal are the result of solidification and melting of crust conductor nodes in the early stages of the experiments (up to around 2 hours), and later due to the solidification and melting of freeze lining conductor nodes.

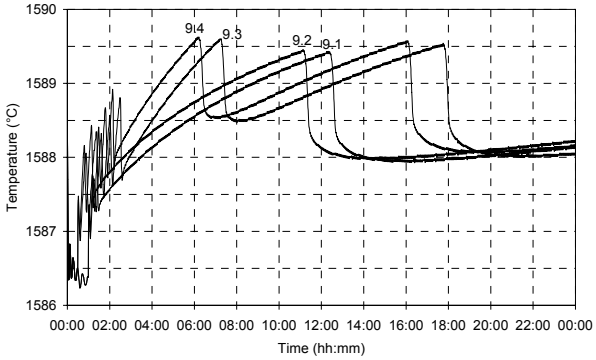

Figure 157 – Chapter 9 summary of variation in slag bath temperature.

9.4.7 Slag Bath Composition

The variation in slag bath composition is shown in graphs (g) and (h) of the experimental results. Graph (g) indicates something that had not been observed up to this point. During the period of solidification the slag TiO_2 content increased and the Ti_2O_3 content decreased. This is consistent with observations made in CHAPTER 6. The FeO content of the slag, however, decreased during solidification while it increased during experiments presented in CHAPTER 6.

The reason for the drop in FeO in the liquid slag can be attributed to reduction taking place at the interface between the slag and metal baths. Reduction reactions at this interface act with solidification to change the slag bath's composition. In the case of FeO, the reduction was dominant. In the case of TiO_2 and Ti_2O_3, solidification was dominant.